Mining, Metallurgy & Exploration (2022) 39:2001–2010
https://doi.org/10.1007/s42461-022-00673-2

Analysis of Steel Prop Supports Subjected to Vertical and Lateral Loading

Khaled Mohamed[1] · **Timothy Batchler**[1]

Received: 26 August 2021 / Accepted: 17 August 2022 / Published online: 10 September 2022
This is a U.S. Government work and not under copyright protection in the US; foreign copyright protection may apply 2022

Abstract
Standing supports have been used in coal mines for decades to enhance roof support capability. Sometimes standing supports are used as a tool to resist the lateral movement of spalled ribs. Researchers from the National Institute for Occupational Safety and Health (NIOSH) are conducting a testing program for different types of standing supports (steel and timber) to investigate the effect of lateral loading on their vertical loading capacities and the factors affecting their lateral loading capacities. In this paper, the mine roof simulator (MRS), at the NIOSH Pittsburgh research facility, was used to determine the response of steel props to vertical and horizontal loadings. Finite element models (FEMs) were developed and verified using the tested steel props. To justify the testing program for testing standing supports with end-conditions of rock-like materials, the verified prop models were used to study the effect of a wide range of roof and floor materials (gray shale, shale, and claystone) on the critical buckling loads of the steel props. Also, several lateral loading scenarios were evaluated in which the steel props were laterally loaded at different heights. The critical buckling load for steel props setting up against a claystone roof and floor was found to be one-half of that shown by the MRS test where roof and floor platens are made of steel. Minimum prop performance was observed when the lateral load was applied at the mid-height of the steel prop, especially at small lateral displacement (less than 2 in).

Keywords Steel props · Coal ribs · Buckling · Lateral loading

1 Introduction

Over the past decade, rib falls resulted in 16 fatalities, representing over 50% of the ground-fall fatalities in U.S. underground coal mines. Statistical analyses on the fatality cases resulting from underground coal pillar rib falls from 2010 to 2019 show that more than 70% of the accidents occurred during the development loading [1]. More recently, the falls of rib or face led to all three of the ground-fall-related fatalities in 2018 and 2019.

Mine operators' decisions concerning rib control and support guidelines are based on the Roof Control Plan Approval and Review Procedures Handbook [2]. Appendix O in this handbook provides information on the conditions that contribute to rib fall hazards and the available methods for protecting miners from rib falls. In fact, the design of rib supports in U.S. underground coal mines is based primarily on local practices and experience, rather than on the engineering design process to manage and control rib hazards. The current rib supports fall into two main categories: rib control based on intrinsic supports and rib control based on external supports [3]. The intrinsic, or rib-bolt support, requires a roof bolting machine that can install a bolt fixture into the rib. Rib control with external supports could be achieved by stabilizing fractured rib through (1) controlling roof-to-floor convergence, (2) restraining detached rib slabs, or (3) providing additional confinement for spalled rib and impeding further rib failure when mesh is used. In some situations—such as unexpected rib sloughing when roof bolters are not available, prop-type standing supports could be the only choice to stabilize fractured ribs. When prop supports are used for rib control, it is very important that they be secured in such a manner that a hazard is not created because of dislodged supports.

Using inappropriate standing support design to control rib sloughing could lead to serious injuries and sometimes fatalities. For example, in a room-and-pillar mine,

✉ Khaled Mohamed
Kmy1@cdc.gov

[1] CDC NIOSH, Pittsburgh, PA, USA

an operator of a continues miner was killed when the victim was struck by a fallen rib. At the incident site, no rib supports of any type were installed for this hazardous rib. In most areas, timbers had been set adjacent to bad ribs, which did not control or prevent the ribs from falling [4]. Also, ignoring the importance of lateral loading capacity of standing support as a factor that could determine the stability of standing support could lead to serious outcomes. For example, in a room-and-pillar mine, roof jacks dislodged by a fallen rib fall and one of the jacks struck a miner, resulting in fatal injuries [5]. The primary failure mechanism of wood crib supports is buckling [6]. Instability of the crib occurs when the support is incapable of transmitting induced vertical and horizontal forces through their structure to create the necessary force couples to maintain moment equilibrium. These moments induce buckling of the structure. It seems reasonable then that those shorter cribs will have less capacity when subjected to horizontal displacements once the critical buckling strength is reached. This behavior can also be addressed by physical observation of the curvature (profile) of the structure. At higher heights, the curvature, which is a measure of moment, is less than it would be for shorter heights for the same horizontal displacement.

The mine roof simulator (MRS) is a unique load frame that provides for efficient product development and performance evaluation that closely simulates the in-service load conditions in the underground coal mines. Since the 1980s, the MRS has been used for decades to test the response (strength, stiffness, and stability) of various support systems for a wide range of load scenarios: uniform vertical loading, asymmetric vertical loading, biaxial loading [7]. To the best of the authors' knowledge, minimal research has been done to assess the performance characteristics of standing support systems for resisting lateral load and for those used to contain rib sloughing. Previous research investigated the effect of horizontal displacements (simulating floor heave) on wood crib stability by controlled biaxial displacement of full-scale wood crib supports [8].

The National Institute for Occupational Safety and Health (NIOSH) is currently developing a design methodology for evaluating rib support based on the inherent stability of the coal ribs and support methods (intrinsic and external) [9]. A testing program for standing supports is underway to provide an engineering-based design method for standing support as rib control tools. The testing program will provide information regarding the lateral loading capacity of different types of standing supports from different manufacturers. The key factors affecting the response of standing supports subjected to lateral loading will be studied. These factors are the type of standing support (steel and timber), support geometry (shape, dimension), support structure (single-component or multiple-components), spatial location of the lateral load along the support, and end-conditions of support (rock strength).

2 Problem Description and Methodology

In this paper, the following questions concerning single-component steel props are addressed:

i. Do the end-conditions of steel prop affect its vertical loading capacity?
ii. Does the spatial location of the lateral load along the support affect its lateral loading capacity?

The application of the MRS test facility has been extended to include lateral testing for standing supports to evaluate the lateral loading capacity of standing supports. The response of steel props of different heights was studied under vertical and lateral loadings. Finite element models were developed and verified using the tested steel props. The verified model was used to answer the preceding questions and to justify the need for initiating a testing program using the MRS for testing standing supports with rock-like roof and floor end-conditions.

3 Full-Scale Testing for Steel Props

This study conducted full-scale buckling and lateral loading testing for steel props using the MRS. The props are ASTM A500 Welded Grade C pipes. The outside diameter and wall thickness of the pipes were 3.5 in and 0.25 in, respectively.

Full-scale testing of steel props represents the real condition in coal mines, especially when synthetic rock foundations will be included in the future tests. The plan is to conduct full-scale tests for different prop types to study the effects of end-conditions (rigid steel platens and soft synesthetic rock) on both vertical and lateral loading capacities of props. The cost of testing full-scale test specimens can increase significantly due to the number of test specimens, laboratory staff, and cost to run equipment. Also, the test site availability is very limited due to the unique capabilities and demand of the MRS. Therefore, for the primary study conducted in this paper, a limited number of full-scale prop tests were conducted.

3.1 Vertical Load Capacity Tests

The objective of this test is to establish a baseline performance for the tested steel props under vertical loading. Three steel props were of different heights (6 ft, 7 ft, and 8 ft).

The steel prop was placed in the MRS with full roof and floor contact to establish uniform loading on the support. To simulate the convergence of the mine roof and floor, a controlled vertical displacement was applied at a rate of 0.05 in/min to the prop by the load frame. Figure 1 shows an 8-ft prop that is straight before testing but buckled around the mid-height after testing.

The convergence of roof and floor platens of the MRS continued until the prop became unstable; then, the prop was unloaded gradually. Figure 2 shows the results of the steel prop tests. Test A was for a 6-ft-tall prop with a peak vertical load of 191 kips at 0.34 in of convergence. Test B was for a 7-ft-tall prop with a peak vertical load of 169 kips at 0.28 in of convergence. Test C was for an 8-ft prop with a peak vertical load of 148 kips at 0.28 in of convergence.

(a) before testing (b) after testing

Fig. 1 An 8-ft height prop

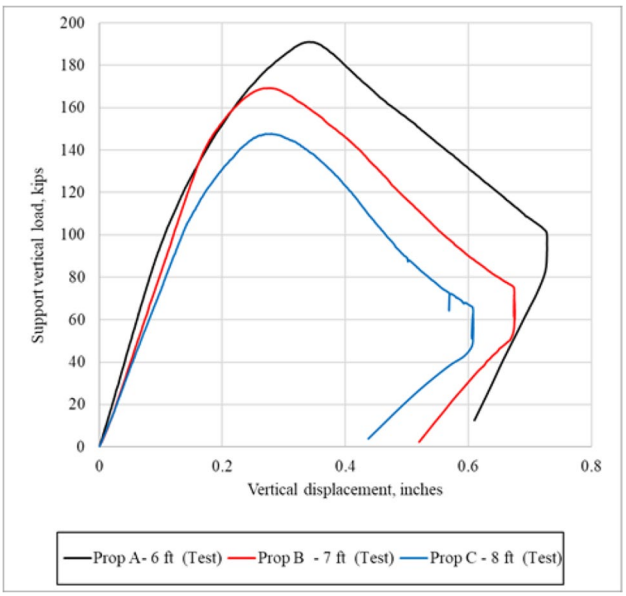

Fig. 2 Vertical load-displacement curves for three prop heights

3.2 Lateral Load Capacity Tests

The testing of steel props for lateral load capacity was also conducted in the MRS. A lateral loading fixture attached into the floor platen of the MRS (shown in Fig. 3) was used to apply lateral loading on tested steel props. The lateral load was applied via a hydraulic cylinder mounted on the lateral loading frame. The height of the fixture is about 6 ft tall, and the position of the hydraulic cylinder is adjustable so that the lateral load can be applied at the mid-height of the test specimen.

Two 8-ft-tall steel props were tested. Each prop was an ASTM A500 Welded Grade C prop with an outside diameter of 3.5 in and a wall thickness of 0.25 in (same as the vertical tests mentioned above). In the first test (prop L1), plywood boards of 0.5-in thickness were placed at the top and base of the prop, and then, the prop was loaded vertically with a very small axial load of 13 kips (Fig. 3a). Then, the prop was loaded horizontally until it slipped (Fig. 3b). In the second test (prop L2), plywood boards of 0.5-in thickness were placed at the top and base of the prop, and the prop was restrained from horizontal movement at its ends with steel blocks at the top and base of the prop (Fig. 4). The prop was preloaded vertically with 20 kips (Fig. 4a); then, the prop was loaded horizontally until it was deformed and became unstable (as shown in Fig. 4b).

Figure 5 shows the lateral loading results of the tested steel props. Test prop L1 with a preload of 13 kips and only frictional restraint at support boundaries exhibited a peak lateral load of 6.3 kips at 1.15 in of prop deflection. The initial vertical loading of Test L1 was not maintained during the test due to the low vertical loading, possibly within the range of MRS accuracy. The lateral loading was much better controlled because it was measured via a load cell.

Test L2, with a preload of 20 kips and a restraint with steel blocks at support boundaries, exhibited a peak lateral load of 10.79 kips at 3.57 in of prop deflection. When the prop pushes laterally, it bends and forms an arch between the MRS platens. This arching mechanism with stationary MRS platens explains the ability of support L2 to maintain about 13 kips of lateral load while the vertical load was zero (Fig. 5).

4 FEM Model for the Tested Steel Props

Finite element models were created for tested props and compared with MRS results. The elastic and yielding properties of the tested props are required to build the

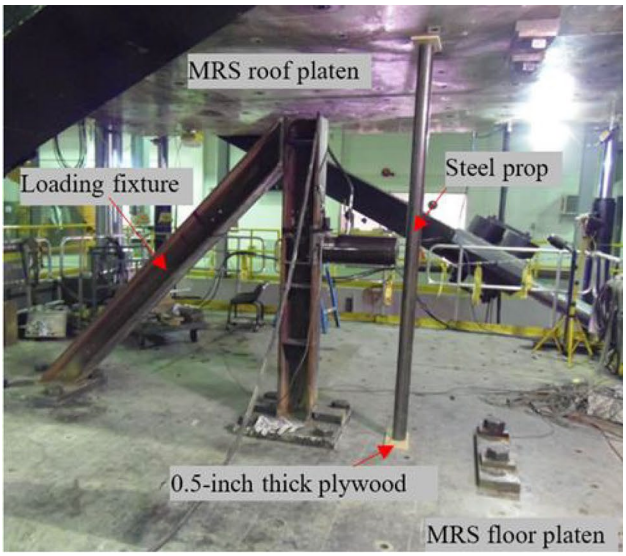

(a) Prop (L1) before testing

(b) Prop (L1) after testing

Fig. 3 Prop (L1) preloaded vertically with 13 kips

numerical models. Young's modulus and Poison's ratio of the ASTM A500 Welded Grade C pipe are 28×10^6 psi and 0.3, respectively. The rated yield strength of the steel pipe is 46 ksi. The nonlinear stress–strain relationship of the pipe, illustrated in Fig. 6, was calculated using the generalized Ramberg–Osgood equation (Eq. 1) and assuming that the yield stress be at 0.2% offset strain [10].

Fig. 4 Prop (L2) preloaded vertically with 20 kips

(a) Prop (L2) before testing

(b) Prop (L2) after testing

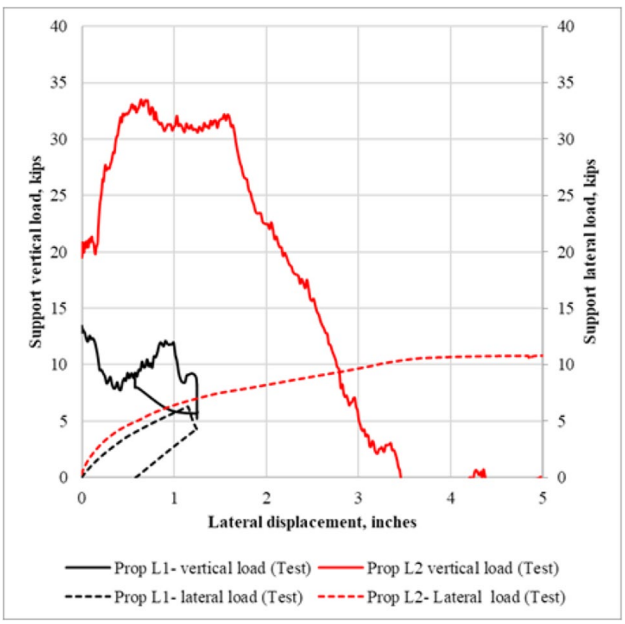

Fig. 5 Vertical and lateral support loads versus lateral support displacement curves for two steel props of 13 kips and 20 kips vertical preloads

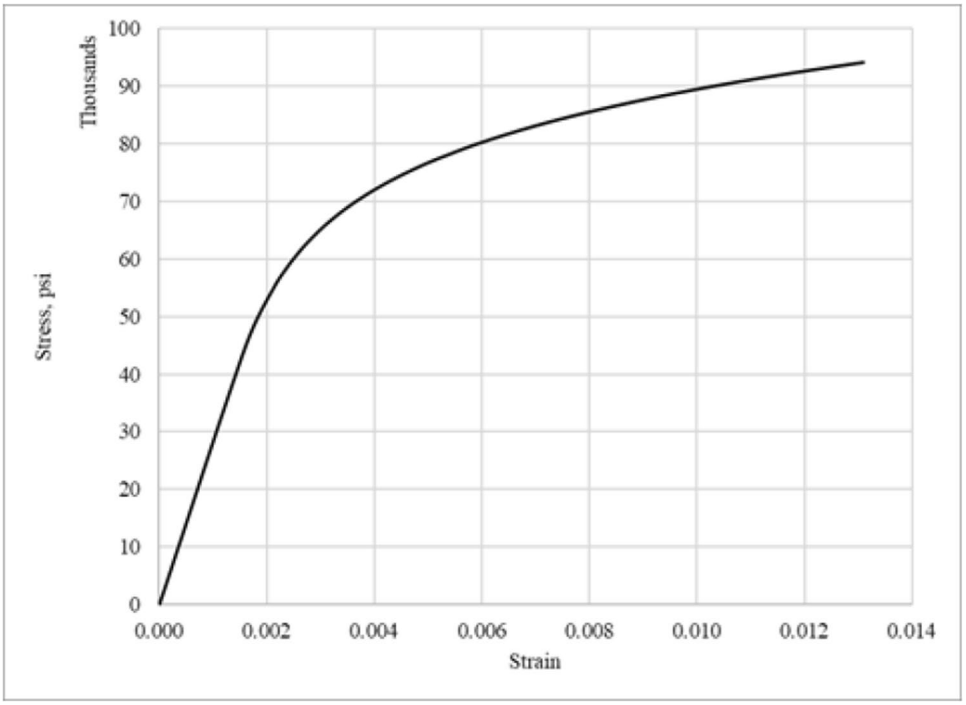

Fig. 6 Stress–strain curve of ASTM A500 Welded Grade C pipe

$$\varepsilon = \frac{\sigma}{E} + 0.002 \times \left(\frac{\sigma}{\sigma_{YS}}\right)^{1/n} \quad (1)$$

where.

σ is the stress in psi.

ε is the strain.

E is Young's modulus in psi.

σ_{YS} is the yield strength in psi.

n is a constant describing the hardening behavior of the material. Best match between finite element models and buckling tests for steel props was achieved by assuming n constant equals to 0.143.

The ANSYS [11] finite element models were developed to simulate the loading and deformation behaviors of the steel props. Figure 7 shows the model configurations for simulating steel props subjected to vertical and horizontal loadings in the MRS. The model consists of three main parts—roof steel platen, prop, and floor steel platen.

For simulating steel props subjected to lateral loading, steel blocks are bonded to the roof and floor platens to constrain the lateral movement of the prop at its ends. The plywood boards (see Figs. 3 and 4) were not included in the models. The lateral loading frame was simplified in the models by applying the lateral load on the prop via a steel pusher block (Fig. 7b). The roof platen was fully constrained, while the floor platen was constrained in the x-direction and z-direction. Steel props are loaded vertically by moving the floor platen in the y-direction. The steel pusher is constrained in the y-direction and

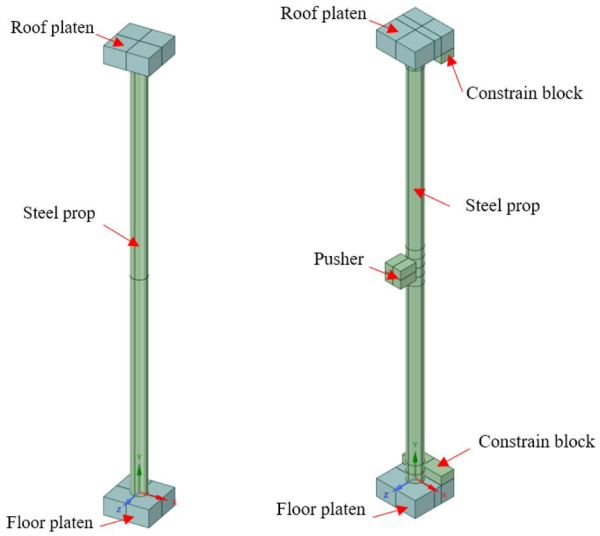

(a) vertical loading (b) lateral loading

Fig. 7 Finite element model configurations

z-direction, and it is free to move in the x-direction to apply lateral load on the steel prop. A friction coefficient of 0.5 was assigned for the contacts between the steel props and both pusher and platens (Fig. 7). Elastic steel properties were assigned to all parts of the model, except the steel prop. Nonlinear stress–strain (see Fig. 6) was assigned for the steel prop in the finite element model.

4.1 Verification of the Steel Prop Model Using Vertical Loading Tests

Compression members, like steel props, could fail by one of two mechanisms: material failure or structural instability, which is often called buckling. Predicting prop failure was determined using finite element models, in which the prop was loaded gradually by displacing the floor platen until maximum vertical support capacity was achieved. The models assumed perfect prop geometry to eliminate the prop buckling mechanism. Figure 8 shows measured and finite element modeling (without buckling) load–displacement curves for three prop heights. It shows that the FE model of steel prop successfully calculated the load–displacement relationships up to the measured peak loads. The ultimate load capacity of the simulated steel props is 229 kips, which is about 20% to 50% more than the measured support loads. This means the three steel props were failed by buckling, not by material failure.

The Euler buckling theory can be used to predict buckling for slender or thin-walled components under compressive stress. The Euler buckling theory is valid if the standing has a slenderness ratio that obeys the following inequality:

$$\text{Slenderness ratio of long prop} > \sqrt{\left(\pi^2 \times E/\sigma_u\right)} \tag{2}$$

where E and σ_u are the Young modulus and ultimate strength of steel prop. Therefore, tested steel props will be classified as long props if their slenderness ratio is greater than 56.

The slenderness ratio was calculated for the tested steel props using the following equation:

$$\text{Slenderness ratio} = \frac{k \times L}{\sqrt{\frac{A}{I}}} \tag{3}$$

where,

k is a constant that depends on the restraints of the two ends of the steel prop, and k equals 0.5 for tested steel props,

L is the length of the steel prop, and,

I and A are the area moment of inertia and area of the cross-section of the steel prop.

The calculated slenderness ratios for the 6-ft, 7-ft, and 8-ft props are 31, 36, and 42, respectively. Therefore, Euler buckling is not applicable to predict the buckling of tested steel props. Alternatively, finite element modeling can be used to calculate the critical buckling loads for the tested steel props.

Typically, the onset of buckling takes place in the elastic range, but for the tested steel props the onset of buckling can take place in the plastic range. To study the

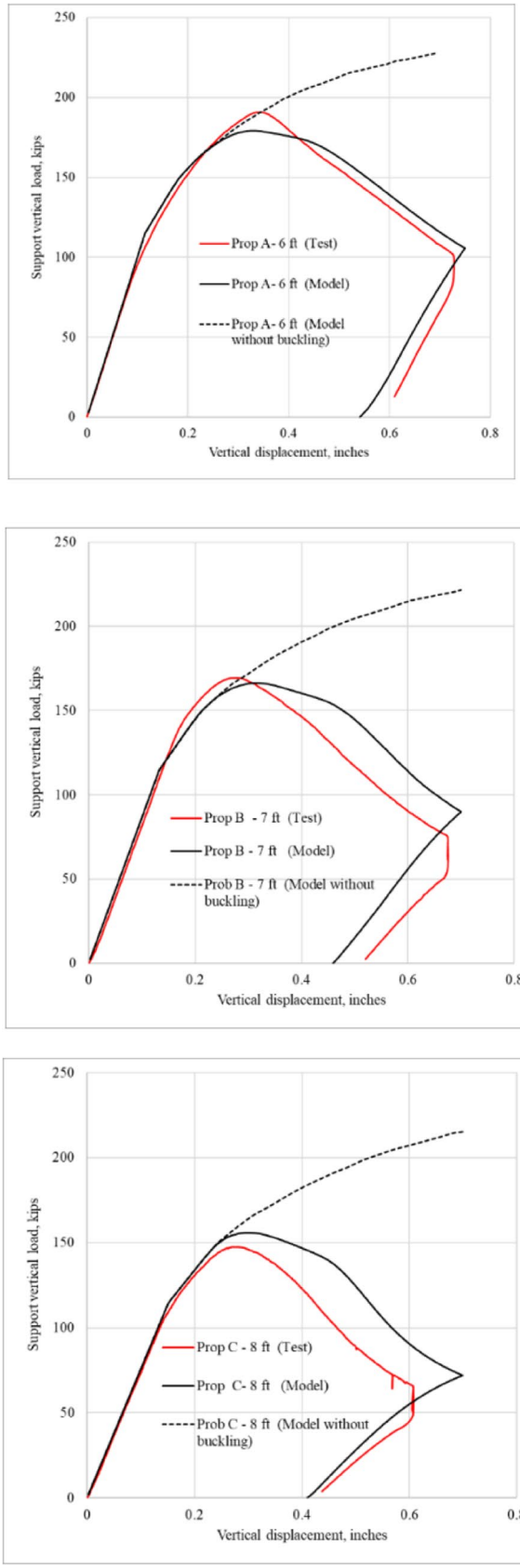

Fig. 8 Experimental and finite element modeling load–displacement curves for three prop heights

buckling behavior of the tested steel props in the plastic range along with nonlinear geometry considerations, imperfection in the geometry of the modeled steel props was imposed to promote prop buckling. Figure 9 shows the deformed shape of the modeled prop compared with the prop after testing. It shows that the deformed shape of the prop model is very similar to the deformed shape of the tested steel prop.

Figure 8 shows the modeling results of the three buckled prop models (solid black curves) compared with the corresponding test results (solid red curves). Prop A of a 6-ft-tall prop has a peak vertical load of 179 kips at 0.33 in of convergence. Model B of a 7-ft-tall prop has a peak vertical load of 166 kips at 0.31 in of convergence. Model C of an 8-ft-tall prop has a peak vertical load of 156 kips at 0.30 in of convergence.

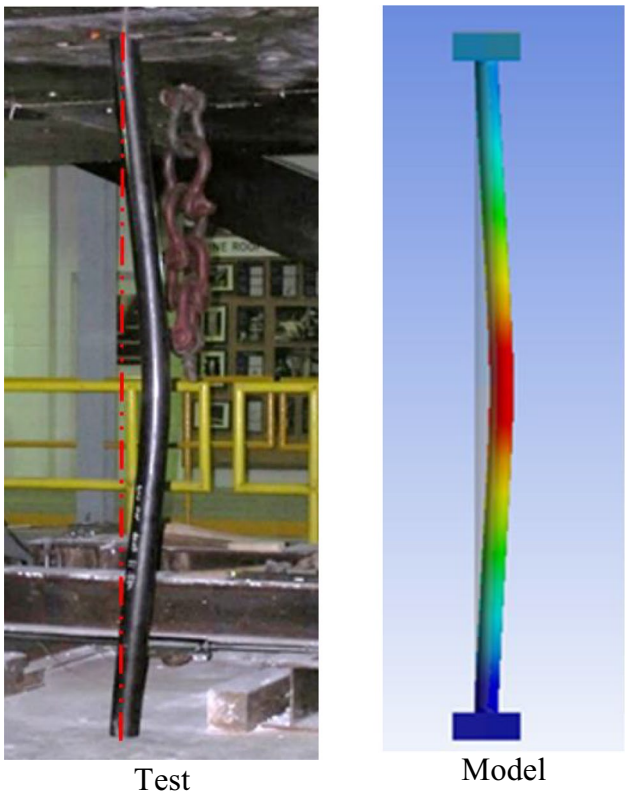

Fig. 9 Deformed shape of prop model, loaded vertically, compared with test results

Table 1 summarizes the measured and calculated critical buckling loads and corresponding vertical displacements. It shows that the prop model successfully calculated the critical buckling load for the tested prop with an error of 6% at maximum.

4.2 Verification of the Steel Prop Model Using Lateral Loading Tests

Finite element modeling was used to calculate the lateral loading capacity for tested steel props L1 and L2 as a result of lateral displacement at their mid-heights. Figure 10 shows the deformed shape of the modeled prop compared with the prop after testing. It shows that the deformed shape of the prop model is very similar to the deformed shape of the tested steel prop. The deformed model clearly shows the rotations of prop ends and the development of arch action in the prop model.

Figure 11 shows the modeling results of the prop models compared with the corresponding test results. It shows the vertical and lateral support loads versus lateral displacement of the prop at its mid-height. As mentioned earlier, the 0.5-in-thick plywood boards at the top and base of the prop model were ignored in the simulation. Because of that, the support vertical loads were overpredicted, especially for prop L1 with a small preload of about 13 kips. The predicted lateral load capacities for prop L1 and prop L2 agree with test results (see red curves in Fig. 11).

5 Factors Affecting Lateral Loading Capacity of Steel Props

The verified FE steel prop model was used to study the effects of end-conditions on the vertical loading capacity of steel props. The effects of roof-to-floor convergence and the spatial location of the lateral load along the prop on the lateral loading capacity of steel props were studied using the verified FE steel prop model.

The roof and floor of the MRS are made of steel, which is about 20 times stiffer than the roof and floor rocks in underground coal mines. The responses of steel props were modeled assuming different types of roof and materials—steel, gray shale, shale, and claystone. The

Table 1 Critical buckling load and corresponding vertical displacement

Prop height, ft	Critical buckling load, kips			Vertical displacement at critical load, in		
	Test	Model	Error %	Test	Model	Error %
6	191	179	−6%	0.34	0.33	−3%
7	169	166	−2%	0.28	0.31	13%
8	148	156	6%	0.28	0.30	7%

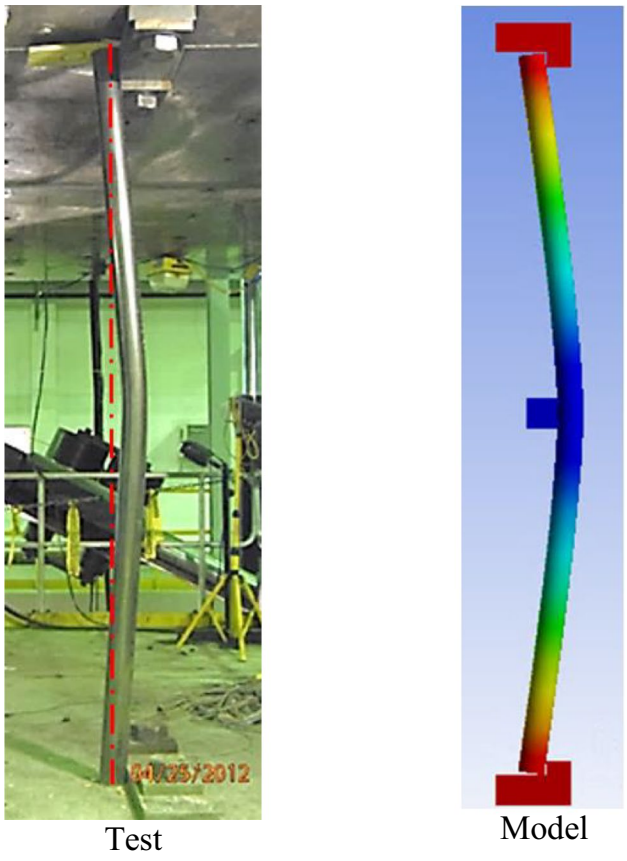

Fig. 10 Deformed shape of prop model compared with test results of prop L2

material properties of the roof and floor materials are summarized in Table 2 [12].

Figure 12 shows the modeling results of the 8-ft prop models for different roof and floor materials. It shows that the elastic stiffness of the prop with claystone rocks was about half the stiffness of the prop with steel roof and floor material. Likewise, the maximum support load with claystone rocks was about 60% of the peak support load of steel props with steel roof and floor material. Figure 12 also shows that the effect of roof and floor material on the prop response became insignificant at large roof-to-floor convergence (about 0.6 in).

In the field, lateral support loading could happen at any heights along the standing support. Therefore, several lateral loading scenarios were assumed in which the prop was laterally loaded at different positions: 0.1, 0.2, 0.3, 0.4, and 0.5 of prop height (see Fig. 13). For slight lateral displacement, less than 0.5 in, the greatest lateral loading capacity was observed when the lateral load was applied near the prop ends, at about 0.1 prop height. The smallest lateral loading capacity of the support was observed at the mid-height of the steel prop. At higher lateral displacement, from 1 to 2 in, the greatest lateral loading capacity was observed at about 0.2 prop height.

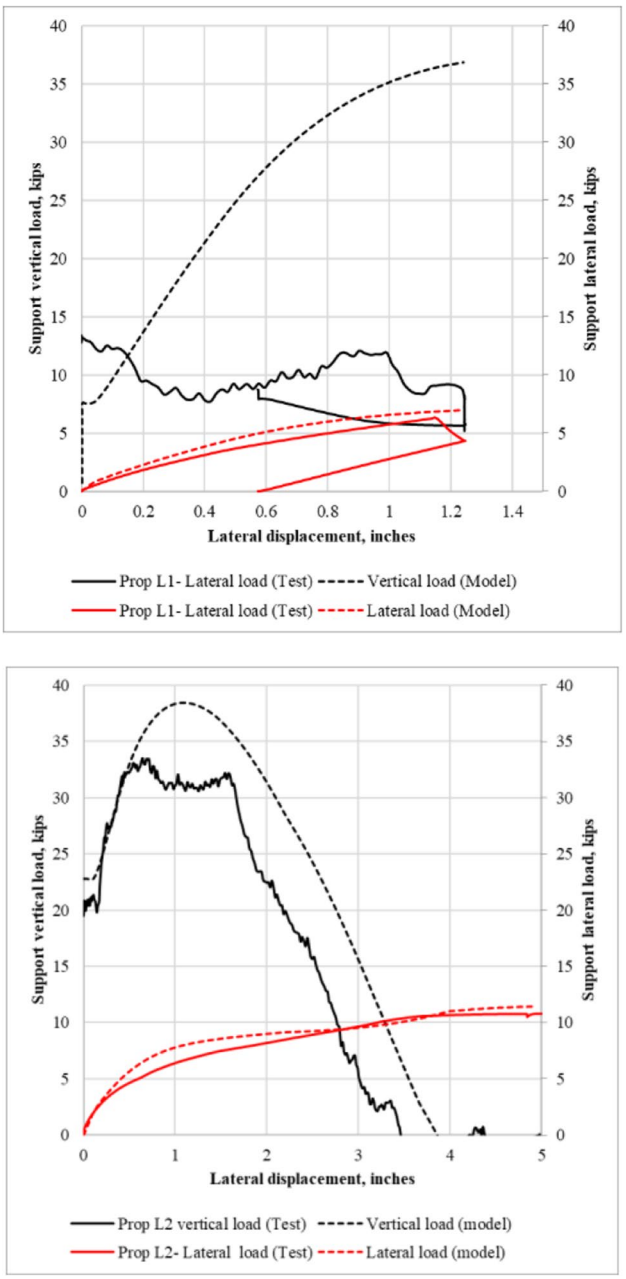

Fig. 11 Experimental and finite element (FE) modeling load–displacement curves for steel props L1 and L2

At a ratio of 0.1, the line of action of horizontal load was very close to the prop's end (support); therefore, the moment was very small at the early stage of loading (~ 0.2 in.). But with further loading, a sudden movement was observed at the end of the prop (support). For very high lateral displacement, greater than 4 in, the effect of the position of lateral loading on the lateral loading capacity became irrelevant. These observations are useful in determining the optimal height at which the external standing support is in contact with the rib.

Table 2 Roof and floor material input parameters

	Young's modulus, psi × 10^6	Poisson ratio	Cohesion, psi	Friction angle, deg	Dilation angle, deg
Gray-shale	1.02	0.31	870	26	26
Shale	0.58	0.31	290	23	23
Clay-stone	0.44	0.31	174	22	22

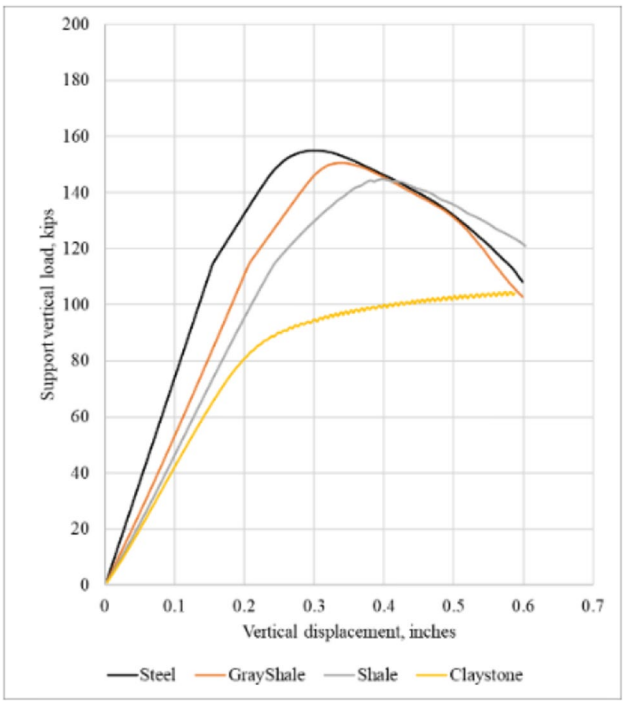

Fig. 12 Finite element modeling load–displacement curves for 8-ft-height prop for different roof and floor materials

6 Summary

The National Institute for Occupational Safety and Health (NIOSH) is conducting this research project to reduce the number of rib-fall accidents in mines by developing an engineering-based design methodology that assesses the performance characteristics of various standing support systems used to contain rib sloughing. This study will provide information regarding the lateral loading capacity of different types of standing supports under full-scale performance testing. From these observations, mining operations can improve their techniques for rib control. The findings discussed in this paper will also help in planning a full-scale testing program for using standing supports as a secondary method for rib control. The key findings of this paper are as follows:

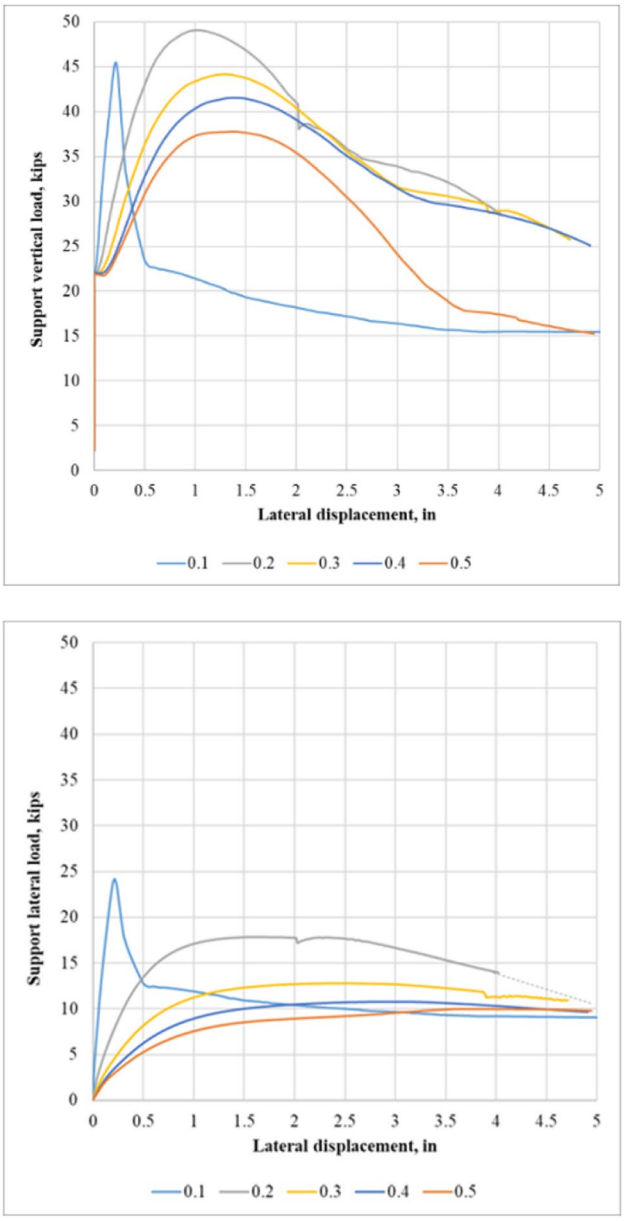

Fig. 13 Finite element (FE) modeling load–displacement curves of prop L2 for different positions of lateral loadings

- The tested steel props failed due to buckling in the process of plastic deformation.

- The modeled elastic stiffness of the steel props setting up against the claystone rocks has a reduced stiffness about half of that tested in the mine roof simulator (MRS).
- The modeled maximum support load with claystone roof and floor rocks was about 60% of that obtained by the MRS test.
- For slight lateral displacement, less than 0.5 in, the greatest lateral loading capacity was observed when the lateral load was applied near prop ends, at about 0.1 prop height. For very high lateral displacement, greater than 4 in, little effect was seen of the position of lateral loading on the lateral loading capacity.

Declarations

Disclaimer The findings and conclusions in this study are those of the authors and do not necessarily represent the official position of the National Institute for Occupational Safety and Health (NIOSH), Centers for Disease Control and Prevention. Mention of any company or product does not constitute endorsement by NIOSH.

Conflict of Interest The authors declare no competing interests.

References

1. MSHA (2019) Accident, illness and injury and employment self-extracting files (part 50 data), 2010–2019. https://arlweb.msha.gov/STATS/PART50/p50y2k/AETABLE.HTM
2. MSHA (2013) Roof control plan approval handbook
3. Mohamed KM, Murphy MM, Lawson HE, Klemetti T (2016) Analysis of the current rib support practices and techniques in U.S. coal mines. Int J Min Sci Technol 26:77–87
4. MSHA (2012) Report of investigations. Fatal rib roll accident. CAI-2012–04
5. MSHA (2010) Report of investigation. Fall of roof/rib. CAI-2010–38
6. Barczak TM, Tasillo CL (1988) Factors affecting the strength and stability of wood cribbing: height, configuration, and horizontal displacement. U.S. Department of Interior, Bureau of Mines, RI 9168, 23 p
7. Barczak TM (1988) An overview of standing roof support practices and developments in the United States. Proceedings of the Third South African Rock Engineering Symposium, Johannesburg, Republic of South Africa: S Afr Inst Min Metall October 10–12, 2005:301–334
8. Barczak TM and Tasillo Carol L (1988) Factors affecting strength and stability of wood cribbing: height, configuration, and horizontal displacement. Report of investigations (United States Bureau of Mines), 9168
9. Mohamed KM, Xue Y, Rashed G, Kimutis R (2021) Analyzing rib stability and support using a coal pillar rib rating. In: 40th International Conference on Ground Control in Mining. Canonsburg, PA, USA
10. Nargund S and Williams DK (2016) Review and comparison of buckling methodologies for ASME B&PV code, section III, subsection NF linear piping restraints. Downloaded From: http://proceedings.asmedigitalcollection.asme.org/. Accessed 11/13/2017
11. ANSYS (2020) Documentation for ANSYS, release 20. ANSYS Inc., Canonsburg, PA
12. Zipf RK (2007) Numerical modeling procedures for practical coal mine design. In: Proceedings of the International Workshop on Rock Mass Classification in Underground Mine Design. National Institute for Occupational Safety and Health, NIOSH IC 9498.

Publisher's Note Springer Nature remains neutral with regard to jurisdictional claims in published maps and institutional affiliations.